Copy of conference proceedings for:

D.S.A. De Focatiis and C.P. Buckley (2012), *A toolbox for parameter-free predictions of solid-state properties of glassy polymers*. 28th International Conference of the Polymer Processing Society, Pattaya, Thailand, 11-15 Dec 2012.

Main journal article relating to this conference paper:

D.S.A. De Focatiis and C.P. Buckley (2012), *A toolbox for parameter-free predictions of solid-state properties of monodisperse glassy polymers with frozen-in molecular orientation*, Journal of Polymer Science Part B: Polymer Physics, 50, pp 1748–1756. doi: 10.1002/polb.23196

Other related journal articles:

D.S.A. De Focatiis and C.P. Buckley (2011), *Craze initiation in glassy polymers: quantifying the influence of molecular orientation*, Polymer, 52 (18), pp 4045-4053. doi: 10.1016/j.polymer.2011.06.044

D.S.A. De Focatiis and C.P. Buckley (2011), *Prediction of frozen-in birefringence in oriented glassy polymers using a molecularly-aware constitutive model allowing for finite molecular extensibility*, Macromolecules, 44 (8), pp 3085–3095. doi: 10.1021/ma102906z

D.S.A. De Focatiis, J. Embery and C.P. Buckley (2010), *Large deformations in oriented polymer glasses: experimental study and a new glass-melt constitutive model*. Journal of Polymer Science Part B: Polymer Physics, 48 (13), pp 1449-1463. doi: 10.1002/polb.22028

davide.defocatiis@nottingham.ac.uk

A TOOLBOX FOR PARAMETER-FREE PREDICTIONS OF SOLID-STATE PROPERTIES OF ORIENTED GLASSY POLYMERS

D.S.A. De Focatiis[1*] **and C.P. Buckley**[2]
[1]*Division of Materials, Mechanics, and Structures, University of Nottingham, UK – davide.defocatiis@nottingham.ac.uk*
[2]*Department of Engineering Science, University of Oxford, UK – paul.buckley@eng.ox.ac.uk*

Abstract – The focus of this study is to develop genuinely parameter-free predictive capability for solid-state properties of melt-processed glassy polymers. A toolbox is assembled from a previously proposed melt-solid constitutive model that provides the necessary residual stress components required for predictions of birefringence and craze initiation stress. The Likhtman-McLeish theory for linear rheology of entangled polymers is employed to generate the low reduced frequency part of the linear viscoelastic spectrum, the only molar mass dependent input parameter. All other parameters are obtained by experiment or from literature, and can be considered material constants. Toolbox predictions are compared to new experimental data on two grades of linear monodisperse polystyrene of known molar mass but unknown rheology and to literature data, and can account for the role of molar mass on birefringence and craze initiation stress of polystyrenes subjected to supra-entanglement orientation processes.

Keywords: polystyrene, orientation, constitutive model, birefringence, crazing.

Introduction

Polymer processing engineers are well versed with both intentional and unintentional frozen-in molecular orientation arising in polymeric products as a direct consequence of flow processes during melt-processing. Orientation leads to anisotropy in Young's modulus [1], yield stress [2, 3], crazing stress [4, 5], optical birefringence [2, 6, 7], strain-hardening modulus [8, 9] and fracture toughness [10], and these properties are sensitive to both the grade of polymer employed and to the flow history encountered [5, 7, 8].

The present authors recently proposed a fully 3-D constitutive model for predicting the non-linear melt-state and solid-state constitutive response of glassy monodisperse polymers [8]. By fitting this model to the linear viscoelastic spectrum of two monodisperse linear polystyrenes (PS), the authors demonstrated that it is possible to predict the optical birefringence [7], the craze initiation stress [5], and the solid-state mechanical response [8] of a polymer of given molar mass subjected to an arbitrary process history, with a small number of molar mass independent material constants.

For the special case of linear monodisperse polymers, the melt region of the linear viscoelastic spectrum can be predicted accurately with the Likhtman-Mcleish (L-M) theory [11]. Here we tested whether it is possible to employ the L-M theory to replace the rheological experimental data that was previously necessary to provide input to the constitutive model as far as solid-state property predictions are concerned. This critical step enables connectivity between theories whose input parameters are *all* material constants associated with a particular polymer species. The toolbox predictions were compared with experimental data consisting of birefringence and craze initiation stress measurements on two monodisperse PS grades of unknown rheology but significantly different molar mass, subjected to various uniaxial melt orientation processes.

Experimental

The materials studied were two samples of monodisperse linear atactic PS with M_w = 121 kDa (BE) and M_w = 966 kDa (BB) and narrow polydispersities (PDI = $M_w/M_n < 1.1$). An in-house near net-shape moulding technique was employed for the production of parallelepipedic 80 × 6 × 0.5 mm^3 bars [12], and isotropic specimens were produced according to ref. [13].

Oriented specimens were produced by uniaxial melt-drawing in an Instron 5985 testing machine fitted with an environmental chamber, at a range of temperatures T above T_g between 105 °C and 135 °C. All stretching was carried out at a constant crosshead velocity corresponding to a nominal strain rate of 0.02 s^{-1}, to a fixed stretch ratio of $\lambda = 3$. After stretching, specimens were immediately quenched using a cold spray (cooling rate ~15 °C s^{-1}).

Optical birefringence was measured on the central region of the specimens using an Olympus BX51-P transmission optical polarizing microscope fitted with polarizer and compensator under white light [7], and values are reported in Figure 1. Additional experimental data from ref. [7] is also shown.

A previously described technique was employed for the measurement of craze initiation stress of miniature specimens subjected to isochronal 3-point bending creep [14]. Miniature beams approximately $6 \times 2 \times 0.5$ mm^3 were cut from the oriented specimens using a custom jig, soaked in reagent grade diethylene glycol (DEG) for 24 hours, and loaded in 3-point bending creep for 300 s with the beam axis aligned with the orientation direction. After unloading, the length of each crazed region was measured using optical microscopy, allowing determination of the craze initiation stress σ_c. Measurements of $\sigma_c - \sigma_c^{iso}$ (where σ_c^{iso} is the isotropic craze initiation stress) are reported in Figure 2 as averages from a minimum of four beams per experimental condition.

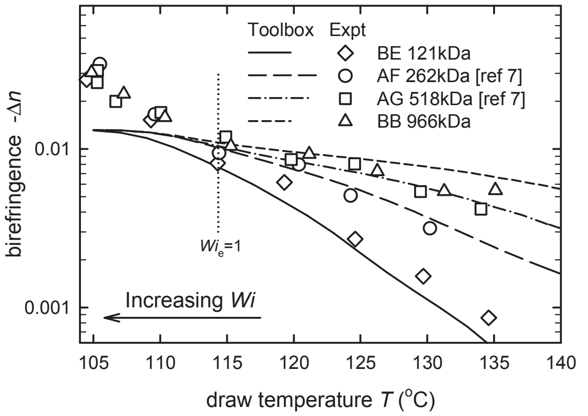

Figure 1 Frozen-in optical birefringence measured on PS specimens melt-drawn at temperature T.

Constitutive model

A constitutive model for the prediction of multiple solid-state properties of glassy polymers with process-induced molecular orientation was developed by the present authors [8], and is shown schematically in Figure 3. It describes the material response to a deformation gradient tensor $\mathbf{F}$ in terms of the Cauchy stress tensor $\boldsymbol{\sigma}$, separated into volumetric $\sigma_{\mathrm{m}} = \frac{1}{3}\operatorname{trace}(\boldsymbol{\sigma}) = K \ln J$ (K is the bulk modulus and $J = \det \mathbf{F}$) and deviatoric $\mathbf{S} = \mathbf{S}_{\mathrm{b}} + \mathbf{S}_{\mathrm{c}}$ parts ($\mathbf{S}_{\mathrm{b}}$ and $\mathbf{S}_{\mathrm{c}}$ are the bond-stretching and conformational contributions respectively). The deviatoric rate of deformation $\bar{\mathbf{D}}$ is given by

$$\bar{\mathbf{D}} = \frac{\hat{\mathbf{S}}_{\mathrm{b},j}}{2G_{\mathrm{b}}} + \frac{\mathbf{S}_{\mathrm{b},j}}{2G_{\mathrm{b}}\tau_j} \tag{1}$$

for each mode j of a spectrum of Maxwell modes. Here $\hat{\mathbf{S}}_j^{\mathrm{b}}$ is the Jaumann rate of stress, G_{b} is the bond-stretching shear modulus, and τ_j is the j th glassy relaxation time. The deviatoric stress is computed as the sum over all M bond-stretching modes, as $\mathbf{S}_{\mathrm{b}} = \sum_{j=1}^{M} \upsilon_j \mathbf{S}_{\mathrm{b},j}$ where υ_j is the relative volume fraction of the j th glassy mode. The reader is referred to refs [15-17] for a more detailed presentation.

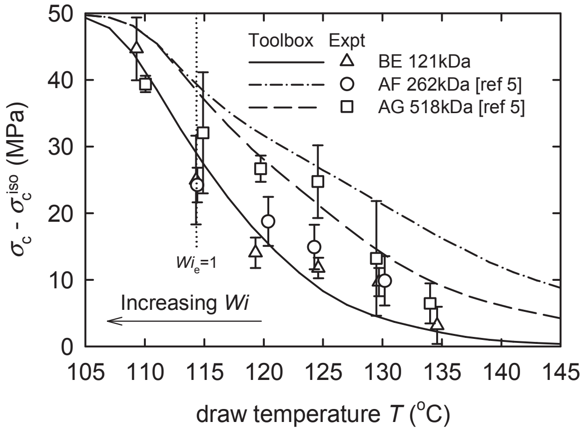

Figure 2 Increase in craze initiation stress relative to isotropic of PS specimens melt-drawn at temperature T. Additional experimental data from ref. [5].

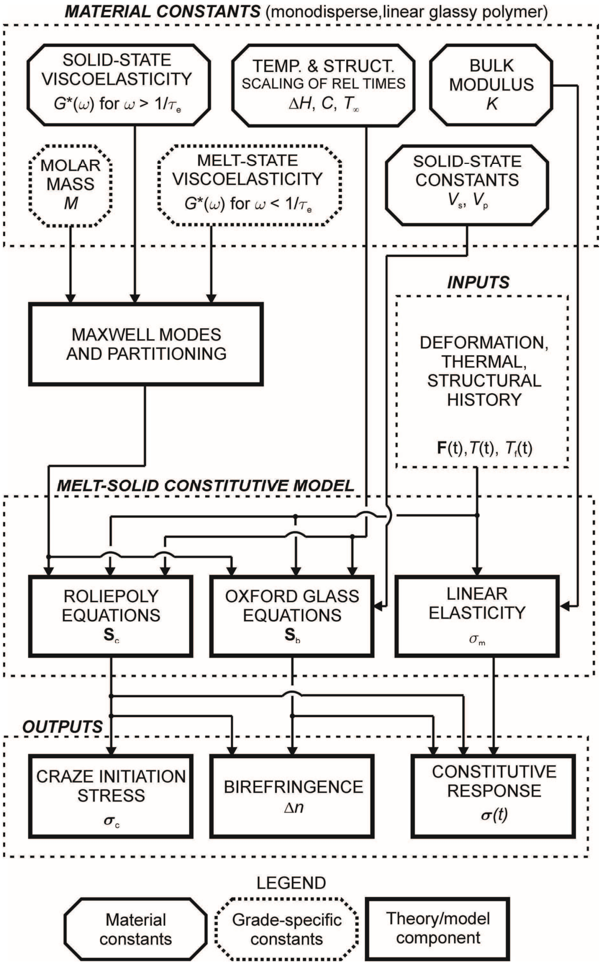

Figure 3 Schematic outline of the toolbox.

The conformational stress is computed from a modified Roliepoly constitutive model that accounts for finite extensibility of chains [7, 18]. A conformational stress is computed for each mode k across a spectrum of N discrete modes by numerical integration of the governing differential equation

$$\begin{aligned} \dot{\mathbf{T}}_k &= \bar{\mathbf{L}} \cdot \mathbf{T}_k + \mathbf{T}_k \cdot \bar{\mathbf{L}}^{\mathrm{T}} - \left(\mathbf{T}_k - \lambda_k^2 \mathbf{I}\right) / \tau_{\mathrm{d},k} \\ &\quad - 2\mathbf{T}_k \left(F(\lambda_k) - 1\right) / \lambda_k \tau_{\mathrm{R},k} \end{aligned} \tag{2}$$

where $\tau_{\mathrm{R},k}$ and $\tau_{\mathrm{d},k}$ are the Rouse and reptation times associated with the k th mode, $\lambda_k = \sqrt{\frac{1}{3}\operatorname{tr}(\mathbf{T}_k)}$ and $F(\lambda_k)$ is a finite chain extensibility correction factor. The conformational stress $\mathbf{S}_{\mathrm{c},k}$ is the deviatoric part of $G_{\mathrm{e}}\left[\mathbf{T}_k F(\lambda_k)/\lambda_k - \mathbf{I}\right]$, where G_{e} is the entanglement modulus. The conformational contribution to the total deviatoric stress is computed as the sum over all N conformational modes, as $\mathbf{S}_{\mathrm{c}} = \sum_{k=1}^{N} \upsilon_k \mathbf{S}_{\mathrm{c,k}}$, where υ_k is the relative volume fraction of the k th Rolie-Poly mode, $\sum_{k=1}^{N} \upsilon_k = 1$.

Rouse and reptation times are referred back to reference values τ^* at a temperature T^* and structural state T_f^* through shift factors a_T and a_struct through $\tau_{\mathrm{R},\,k} = a_\mathrm{T} a_\mathrm{struct} \tau_{\mathrm{R},\,k}^*$ and $\tau_{\mathrm{d,\,k}} = a_\mathrm{T} a_\mathrm{struct} \tau_{\mathrm{d},\,k}^*$. Glassy relaxation times are referred back to reference temperature, structural state and (unstressed) stress state $\tau_{j,0}^*$ through $\tau_j = a_\mathrm{T} a_\mathrm{struct} a_{\sigma,j} \tau_{j,0}^*$ where $a_\mathrm{T} = \exp\left[\left(\Delta H / R\right)\left(1/T - 1/T^*\right)\right]$ (ΔH is the activation enthalpy), $a_\mathrm{struct} = \exp\left[C\left(\left(T_\mathrm{f} - T_\infty\right) - \left(T_\mathrm{f}^* - T_\infty\right)\right)\right]$ (C is the Cohen Turnbull constant, T_f is the fictive temperature and T_∞ is the Vogel temperature), and $a_{\sigma,j} = \left(V_\mathrm{s} \tau_{\mathrm{oct},j}^\mathrm{b} / 2RT\right) \exp\left(-V_\mathrm{p} \sigma_\mathrm{m} / RT\right) / \sinh\left(V_\mathrm{s} \tau_{\mathrm{oct},j}^\mathrm{b} / 2RT\right)$ ($\tau_{\mathrm{oct},j}^\mathrm{b}$ is the octahedral shear stress acting on the j th mode, and V_s and V_p are the shear and pressure activation volumes). In the simulations, we used constants from the literature [8, 19], and the PS was taken to be in equilibrium for temperatures $T \geq 98.9\ ^\circ\mathrm{C}$, and at $T_\mathrm{f} = 98.9\ ^\circ\mathrm{C}$ for $T < 98.9\ ^\circ\mathrm{C}$. G_e (entanglement modulus), M_e and τ_e (molar mass and Rouse time of one entanglement length), were taken as $G_\mathrm{e} = 317.9\ \mathrm{kPa}$, $M_\mathrm{e} = 13.14\ \mathrm{kDa}$ and $\tau_\mathrm{e} = 10.57\ \mathrm{s}$ at $T^* = 120\ ^\circ\mathrm{C}$. λ_max, the finite chain extensibility, was 4.09 [8]. Whole molecule Rouse and reptation times were computed using $Z = M / M_\mathrm{e}$ as $\tau_{\mathrm{R},1}^* = Z^2 \tau^\mathrm{e}$ and $\tau_{\mathrm{d},1}^* = 3Z^3\left(1 - 2.38Z^{-0.5} + 4.17Z^{-1} - 1.55Z^{-1.5}\right)\tau_\mathrm{e}$.

Moduli and relaxation times have previously been obtained by fitting a discrete spectrum of Maxwell modes to a viscoelastic spectrum obtained from experimental data from DMA and shear rheometry [8]. The high frequency part of the spectrum is insensitive to molar mass, but the low frequency linear melt rheology was required to be measured experimentally for each grade, since it is strongly dependent on molar mass. In this toolbox, the linear viscoelastic frequency response was *predicted* directly by the L-M theory for a monodisperse polymer of given molar mass, and hence Z, using the material constants G_e, M_e and τ_e [20]. A discrete relaxation spectrum was then fitted to a combination of the experimental linear viscoelastic data for high frequencies and the theory predictions for low frequencies. Starting at the longest relaxation time, $\tau_\mathrm{d} = \tau_{\mathrm{d},\,1}$, one mode per decade of time was assigned to cover the frequency range of interest using an in-house optimiser. The condition $\sum_{k=1}^{N} G_k = G_\mathrm{e}$ was imposed, restricting Rolie-Poly modes to the conformational response. The viscoelastic spectra of materials BE and BB reconstructed from the Maxwell modes are reproduced in Figure 4.

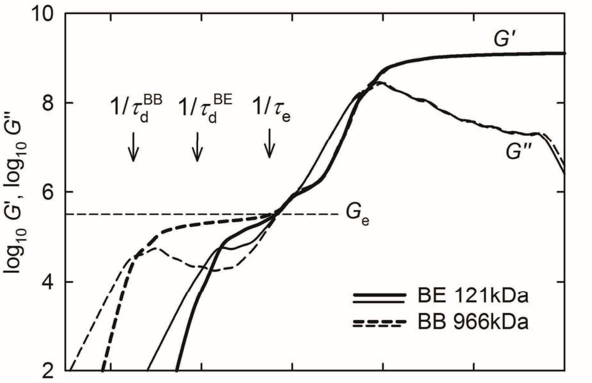

Figure 4 The full linear viscoelastic spectrum for polymers BE and BB used in the simulations.

Results and Discussion

The toolbox is employed to simulate the three stages of the process by which orientation is frozen into the specimens: an isothermal uniaxial orientation through to $\lambda = 3$ at a rate of $\dot{\varepsilon} = 0.02\ \mathrm{s}^{-1}$ for a range of temperatures between $105 - 145\ ^\circ\mathrm{C}$; a fast quench through to $20\ ^\circ\mathrm{C}$ at fixed deformation, at a rate of $15\ ^\circ\mathrm{C\,s}^{-1}$; and a fast unloading through to zero net stress at a deformation rate of $\dot{\varepsilon} = -1\ \mathrm{s}^{-1}$. The simulation predicts a state of self-stress for unloaded oriented specimens in the glassy state, with $\mathbf{S}_\mathrm{b} = -\mathbf{S}_\mathrm{c}$.

Birefringence

Optical birefringence arises from both bond stretching distortions and from conformational alignment of the molecules, and is computed using stress-optical coefficients C_b and C_c ($8.3\times10^{-12}\ \mathrm{Pa}^{-1}$ and $-4.5\times10^{-9}\ \mathrm{Pa}^{-1}$ respectively) as the sum of the two contributions from the in-plane principal bond-stretching and conformational stress differences, ΔS_b and ΔS_c respectively, as

$$\Delta n = C_\mathrm{b} \sum_{j=1}^{M} \upsilon_j \Delta S_{\mathrm{b},j} + C_\mathrm{c} \sum_{k=1}^{N} \upsilon_k \Delta S_{\mathrm{c},k} H\left(\lambda_k / \lambda_\mathrm{max}\right) / H\left(1/\lambda_\mathrm{max}\right)$$

where $H(x) \simeq 1 + x^2/3 + x^4/3$ is a correction factor accounting for finite chain extensibility [7]. Computations of birefringence from toolbox simulations are shown in Figure 1.

The toolbox successfully accounts for the role of molar mass on birefringence, and correctly predicts the increase of Δn with molar mass at a given draw temperature. The numerical values are close to the experimental data for draw temperatures $T \geq 115\ ^\circ\mathrm{C}$ (the drawing regime for which $Wi_\mathrm{e} < 1$). The region on the left ($Wi_\mathrm{e} > 1$) represents drawing with sub-entanglement molecular stretch, and the toolbox underpredicts. This discrepancy highlights the current limitations in the theoretical understanding of orientation processes at very short length scales. Where $Wi_\mathrm{e} < 1$ and supra-entanglement stretch dominates, the average difference between toolbox prediction and experiment is 17%, and is largest at the smallest Δn

values, where there is greatest experimental uncertainty due to the measurement accuracy of the compensator.

Craze initiation stress

In oriented polymers, a back-stress acts to increase the stress required for craze formation σ_{c} relative to the isotropic $\sigma_{\mathrm{c}}^{\mathrm{iso}}$, and this increase is proportional to birefringence for a wide range of orientations [4]. For moderate levels of birefringence the conformational birefringence is directly proportional to the conformational deviatoric back stress, and the increase in crazing stress is given by $\sigma_{\mathrm{c}} - \sigma_{\mathrm{c}}^{\mathrm{iso}} = \Delta S_{\mathrm{c}} / \beta$ where β is a constant, previously determined to be 0.059 ± 0.002 for PS [5]. Thus, knowledge of the frozen-in conformational stress tensor $\mathbf{S}_{\mathrm{c}}$ and of the isotropic craze initiation stress enables predictions of craze initiation stress in uniaxially melt-oriented specimens. This is computed using the toolbox for the full range of experimental orientation temperatures, and is shown in Figure 2.

The toolbox accounts for the role of molar mass on craze initiation stress, and correctly predicts increasing crazing stress with molar mass for a given draw temperature. The predictions also match the experimental observation that the effect of molar mass on craze initiation stress is greatest at intermediate draw temperatures, and smallest at the lowest and highest draw temperatures. At the lowest draw temperatures, relaxation times during melt-drawing are very long, and molecular orientation occurs with little to no relaxation (and hence independently of molar mass). At very high temperatures, there is almost complete relaxation during melt-drawing, and the oriented polymers craze at a similar stress to isotropic polymers of the same molar mass. There is an average difference between toolbox and experiment of 5.8 MPa, or 34% of the matching measured experimental value, across the full range of conditions.

Conclusions

This study has presented a toolbox for the prediction of birefringence and craze initiation stress in oriented monodisperse linear polymers of known molar mass but unknown rheology, using only polymer-dependent material constants and theory. The toolbox was applied to simulations of melt-drawing at a range of temperatures for grades of PS of unknown rheology. Outputs were combined with existing theories to produce predictions of birefringence and of craze initiation stress, and compared to new experimental measurements on two grades of linear monodisperse polystyrene of substantially different molar mass, and to the literature.

The toolbox predictions accounted for all observed experimental trends, and in particular for the role of molar mass on both birefringence and craze initiation. Birefringence predictions were on average within 17% of experimentally measured quantities for all supra-entanglement orientation states and molar masses probed. Crazing predictions were on average within 34% of experimentally measured quantities for the full range of orientations and polymers explored.

Acknowledgements

The authors gratefully acknowledge the contributions of Prof. Mackley of the University of Cambridge, and of Dr Hutchings of the University of Durham for the supply and characterisation of the polystyrenes, and of the Microscale Polymer Processing consortium for helpful discussions. This work was supported by Engineering and Physical Sciences Research Council grant EP/J007978/1.

References

1. H. Wright; C.S.N. Faraday; E.F.T. White; L.R.G. Treloar *J. Phys. D Appl. Phys.*, 1971, 4(12), 2002-2014.
2. A. De Francesco; R.A. Duckett *Polymer*, 2004, 45(23), 8005-8011.
3. E.M. Arruda; M.C. Boyce *Int. J. Plasticity*, 1993, 9(6), 697-720.
4. C. Maestrini; E.J. Kramer *Polymer*, 1991, 32(4), 609-618.
5. D.S.A. De Focatiis; C.P. Buckley *Polymer*, 2011, 52(18), 4045-4053.
6. A. De Francesco; R.A. Duckett *Polymer*, 2004, 45(12), 4297-4306.
7. D.S.A. De Focatiis; C.P. Buckley *Macromolecules*, 2011, 44(8), 3085-3095.
8. D.S.A. De Focatiis; J. Embery; C.P. Buckley *J. Polym. Sci. Pol. Phys.*, 2010, 48(13), 1449-1463.
9. P.J. Hine; A. Duckett; D.J. Read *Macromolecules*, 2007, 40(8), 2782-2790.
10. J. Embery; R.S. Graham; R.A. Duckett; D. Groves; M. Collis; M.R. Mackley; T.C.B. McLeish *J. Polym. Sci. Pol. Phys.*, 2007, 45(4), 377-394.
11. A.E. Likhtman; T.C.B. McLeish *Macromolecules*, 2002, 35(6332-6343.
12. D.S.A. De Focatiis *Polym. Test.*, 2012, 31(4), 550-556.
13. D.S.A. De Focatiis; C.P. Buckley *J. Polym. Sci. Pol. Phys.*, 2012, in press.
14. D.S.A. De Focatiis; C.P. Buckley *Polym. Test.*, 2008, 27(2), 136-145.
15. C.P. Buckley; D.C. Jones *Polymer*, 1995, 36(17), 3301-3312.
16. C.P. Buckley; P.J. Dooling; J. Harding; C. Ruiz *J. Mech. Phys. Solids*, 2004, 52(10), 2355-2377.
17. J.J. Wu; C.P. Buckley *J. Polym. Sci. Pol. Phys.*, 2004, 42(11), 2027-2040.
18. A.E. Likhtman; R.S. Graham *J. Non-Newtonian Fluid Mech.*, 2003, 114(1-12.
19. J.J. Wu; C.P. Buckley *J. Polym. Sci. Pol. Phys.*, 2004, 42(11), 2027-2040.
20. A.E. Likhtman; S.T. Milner; T.C.B. McLeish *Phys. Rev. Lett.*, 2000, 85(4550-4553.